ACS OMEGA

http://pubs.acs.org/journal/acsodf

Article

Energy Decomposition Analysis Coupled with Natural Orbitals for Chemical Valence and Nucleus-Independent Chemical Shift Analysis of Bonding, Stability, and Aromaticity of Functionalized Fulvenes: A Bonding Insight

Sai Manoj N. V. T. Gorantla and Kartik Chandra Mondal*

Cite This: *ACS Omega* 2021, 6, 17798−17810

Read Online

ACCESS | Metrics & More | Article Recommendations | Supporting Information

ABSTRACT: The Donor base ligand-stabilized cyclopentadienyl-carbene compounds L−C_5H_4 (L = H_2C, aAAC; $(CO_2Me)_2C$, Py; aNHC, NHC, PPh_3; SNHC; aAAC = acyclic alkyl(amino) carbene, aNHC = acyclic N-hetero cyclic carbene, NHC = cyclic N-hetero cyclic carbene, SNHC = saturated N-hetero cyclic carbene, Py = pyridine) (**1a-1d**, **2a-2c**, **3**) have been theoretically investigated by energy decomposition analysis coupled with natural orbitals for chemical valence calculation. Among all these compounds, aNHC=C_5H_4 (**2a**) and Ph_3P=C_5H_4 (**2c**) had been reported five decades ago. The bonding analysis of compounds with the general formula L=C_5H_4 (**1a-1d**) [L = (H_2C, aAAC, $(CO_2Me)_2C$, Py] showed that they possess one electron-sharing σ bond and electron-sharing π bond between L and C_5H_4 neutral fragments in their triplet states as expected. Interestingly, the bonding scenarios have completely changed for L = aNHC, NHC, PPh_3, SNHC. The aNHC analogue (**2a**) prefers to form one electron-sharing σ bond (C_L−C_{C5H4}) and dative π bond ($C_L \leftarrow C_{C5H4}$) between cationic $(aNHC)^+$ and anionic $C_5H_4^-$ fragments in their doublet states. Similar bonding scenarios have been observed for NHC (**2b**) and PPh_3 (**2c**) (P_L−C_{C5H4}, $P_L \leftarrow C_{C5H4}$) analogues. In contrast, the SNHC and C_5H_4 neutral fragments of SNHC=C_5H_4 (**3**) prefer to form a dative σ bond ($C_{SNHC} \rightarrow C_{C5H4}$) and a dative π bond ($C_{SNHC} \leftarrow C_{C5H4}$) in their singlet states. The pyridine analogue **1d** is quite different from **2c** from the bonding and aromaticity point of view. The nucleus-independent chemical shifts of all the abovementioned species (**1**−**3**) corresponding to aromaticity have been computed using the gauge-independent atomic orbital approach.

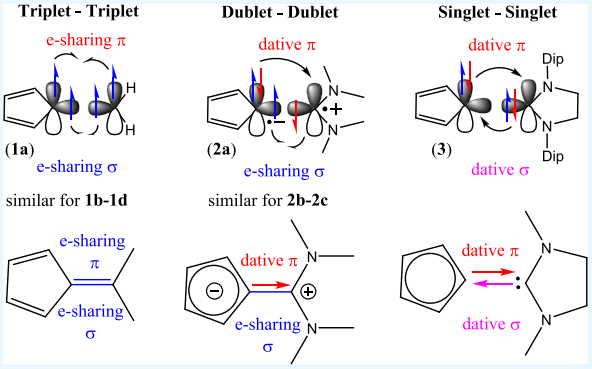

INTRODUCTION

The formation of chemical bonds is one of the uttermost important stabilization forces because of which the atoms/ions/molecules can come close to each other leading to formation of the ingredients of life to the building blocks of megastructures of our universe.[1] The first chemical bond of the universe was a weak dative bond ($He \rightarrow H^+$) between He and H atoms of helium hydride (HeH^+).[1d] Inorganic and organic chemistry started much earlier in space than those on Earth. Up in deep interstellar space, highly polar five-membered ring cyanocyclopentadiene (1-cyano-1,3-cyclopentadiene) has been very recently detected from a combination of laboratory rotational spectroscopy and a sensitive spectral line survey in the radio band toward the starless cloud core.[1e] Cyclopentadiene and cyclopentadienyl rings are among the classic examples of ligands to the chemists. They are regularly utilized in the laboratory for different means.[2−6] Substituted cyclopentadienes/cyclopentadienyls (Cp) are utilized as ligand/groups in different areas of chemistry.[2] They are utilized in organometallic chemistry for the preparation of the catalysts to carry out organic transformations.[3] They have been employed as stabilizing ligand compounds of metalloids and complexes with metal ions and in different oxidation states.[2,4] Some of these functionalized Cp containing molecules/complexes are highly fluorescent,[5] or metal−Cp complexes can display extremely slow relaxation of magnetization.[6] The functionalization of cyclopentadiene/cyclopentadienyl rings with different substituents is very beneficial and demanding. Moreover, the introduction of the imidazolium group might induce ionic liquid properties since imidazolium salts are employed as an ionic liquid for many chemical reactions. Functionalization of

Received: February 4, 2021
Accepted: May 6, 2021
Published: July 6, 2021

ACS Publications

© 2021 The Authors. Published by American Chemical Society

Scheme 1. Representative Types of σ (a–c), π (e–f), Ionic (d), and Charge Shift Bonds (g)[a]

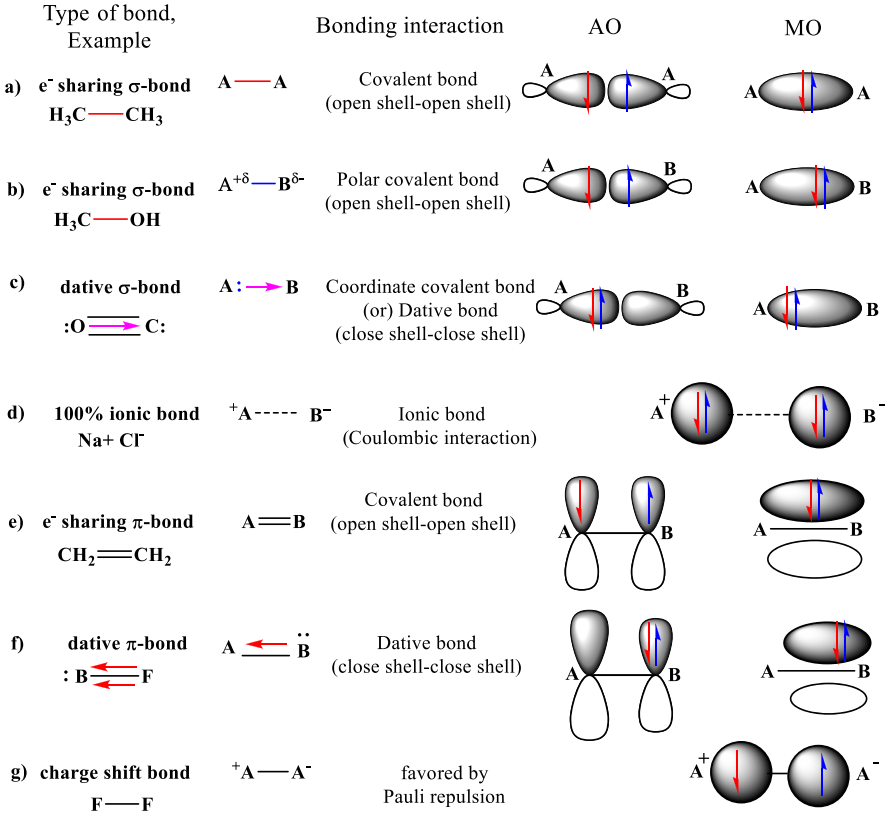

[a]See reference 12 for undisputed use of arrows for dative bonds.

Scheme 2. Donor Ligand-Stabilized C(0) Atom in the Excited Singlet State: Carbodiphosphane $L_2C(0)$ (A); and Monoatomic C(0) Center Acting as Ligands: $L_2C(0) \rightarrow BR_3$ (B) and $L_2C(0) \rightarrow (BR_3)_2$ (C) [L = Ph_3P][a]

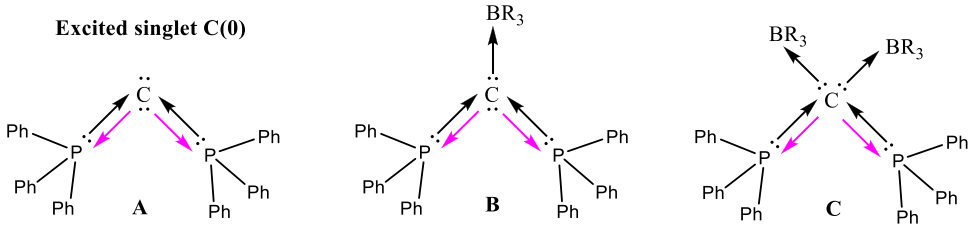

[a]Black and pink arrows represent (→) dative σ bond and dative π bond (R = H).

cyclopentadiene/cyclopentadienyl rings with aliphatic groups of axially bis-ligated Dy-cation efficiently prevents[6] zero-field quantum tunneling via the prevention of intermolecular magnetic interaction (dipolar Cp···Cp interactions).[7] Thus, functionalization of Cp rings with a donor–acceptor neutral ligand [Ph_3P[8a] and $C(NMe_2)_2$],[8b] which started way back in the 1950s, seems to have attracted synthetic chemists till today.[8c−k] The functionalization of the Cp ring with mono- and bis-NHC carbenes (NHC = N-hetero cyclic carbene) started over a decade ago.[8c,d,k] Recent synthetic progress of functionalization of Cp with different carbenes showed that the accumulation of electron densities on the Cp ring is extremely high. The bis-NHC functionalization of Cp leads to the formation of ionic compounds of $[(NHC)_2Cp]^+ X^-$ salts, which rapidly exchange H with D when they have been reacted with D_2O.[8k] The Cp-stabilized half sandwich and sandwich complexes of metalloid and metals have attracted chemists over the past decades.[2−8] The detailed bonding analysis of Cp-functionalized organic molecules is rarely reported.

Gilbert Lewis introduced the Lewis electron pair approach for chemical bonding in 1916. His concept of the cubic electron rule was elaborately popularized by Langmuir in 1919. Langmuir also introduced the octet, 18 e, and 32 e rules and coined the term "covalent bonding" in 1919–1921. Sidgwick suggested an arrow formalism for the coordinate bond in the 1920s. These developments are even before modern quantum theory of bonding. In 1927, Heitler and London explained the physical origin of chemical bonding in H_2, utilizing quantum theory by Heisenberg and Schrödinger. Century-long efforts finally shed light on different bonding scenarios (Scheme 1). The bonding model of Gilbert Lewis has been slightly modified over the years. The rules for using Lewis structures have slightly changed with the flow of time. However, the essential common features of chemical bonding remain the same until today.[9] Even after a century, chemists like to display

https://doi.org/10.1021/acsomega.1c00648
ACS Omega 2021, 6, 17798−17810

the bonding scenarios as a Lewis electron pair. A few decades later, Fukui's frontier molecular orbital (FMO) theory and Woodward and Hoffmann's orbital symmetry rules for pericyclic reactions are significant additions to the bonding and reactivity of organic molecules.[9]

The C atom is at the heart of organic chemistry. Tetravalent and trivalent C compounds most commonly satisfy the octet rule. Carbene with (divalent C atoms) six valence electrons has also been very familiar to organic chemists for over two decades due to its application in metal-free catalysis and also inmetal ion employed catalysis. A less familiar divalent zero-valence C(0)-atom[10] stabilized by two donor ligands Ph_3P (carbodiphosphane; Scheme 2, **A**) was synthesized six decades ago.[10a] The NHC analogue is called carbodicarbene [$L_2C(0)$; L = Ph_3P, NHC].[10c] This monoatomic C(0) of **A** possesses two pairs of electrons that are donatable to the acceptor molecules (Scheme 2, **B** and **C**), which is remarkable. Theoretical calculations[10b] showed that the central C(0) of **A** has been stabilized by donor−acceptor σ and π bonds [L → C, L ← C] with the excited singlet C(0).[10e] Very recently, a linear C_3 unit of $(L)_2C_3$ stabilized by the formation of one electron-sharing σ bond, dative σ bond [C_3^- with $(L)_2^+$; L = Ph_3P, NHC; doublet states], and two dative π bonds (L ← C) has been reported.[11] The arrows for dative bonds were originally used by Sidgwick in 1923.[12a] The use of arrow for a dative bond has been undisputed[12b−d] which was originally envisioned by Sidgwick nearly a century ago.[12a] The same arrow formalism, which was suggested for divalent carbon(0) compounds L → C ← L, was suggested already by Varshavskii in 1980.[13] In past four decades, the quatum chemical calculations on the different aspects of chemical bonding have been significant. Different types of chemical bonds are summarized in Scheme 1 with examples.

Here, we report the theoretical calculations on the stability and bonding of a donor ligand-stabilized C_5H_4 unit having a general formula of $(L)C_5H_4$ (Scheme 1). Our EDA-NOCV analysis shows three different bonding scenarios in these seemingly similar-looking molecules $(L)C_5H_4$ (**1**−**3**) [L = H_2C (**1a**), aAAC (**1b**), $(CO_2Me)_2C$ (**1c**), Py (**1d**); aNHC (**2a**), NHC (**2b**), PPh_3 (**2c**); SNHC (**3**)]. In addition, the computed NICS values have revealed the effect of chemical bonding on the aromaticity of five-membered C_5H_4 rings of all compounds (**1**−**3**).

COMPUTATIONAL METHODS

Geometry optimizations and vibrational frequency calculations of compounds $(L)C_5H_4$ (**1**−**3**) [L = H_2C (**1a**), aAAC (**1b**), $(CO_2Me)_2C$ (**1c**), Py (**1d**); aNHC (**2a**), NHC (**2b**), PPh_3 (**2c**); SNHC (**3**)] in singlet and triplet electronic states have been carried out at the BP86-D3(BJ)/def2-TZVPP level in the gas phase.[14] The absence of imaginary frequencies assures the minima on the potential energy surface. All the calculations have been performed using the Gaussian 16 program package.[15] Natural bond orbital (NBO)[16] calculations have been performed using the NBO 6.0 program[17] to evaluate partial charges, Wiberg bond indices (WBI),[18] and natural bond orbitals. The nature of the bond in L−C_5H_4 compounds was analyzed by energy decomposition analysis (EDA)[19] coupled with natural orbitals for chemical valence (NOCV)[20] using the ADF 2018.105 program package.[21] EDA-NOCV calculations were carried out at the BP86-D3(BJ)/TZ2P[22] level using the geometries optimized at the BP86-D3(BJ)/def2-TZVPP level. The EDA-NOCV method involves the decomposition of the intrinsic interaction energy (ΔE_{int}) between two fragments into four energy components as follows:[23]

$$\Delta E_{int} = \Delta E_{elstat} + \Delta E_{Pauli} + \Delta E_{orb} + \Delta E_{disp} \quad (1)$$

where the electrostatic, ΔE_{elstat} term originates from the quasi-classical electrostatic interaction between the unperturbed charge distributions of the prepared fragments and the Pauli repulsion, ΔE_{Pauli} (repulsion energy due to the interactions of the same spins between the fragments) is the energy change associated with the transformation from the superposition of the unperturbed electron densities of the isolated fragments to the wavefunction, which properly obeys the Pauli principle through explicit anti-symmetrization and renormalization of the production of the wavefunction. The dispersion interaction, ΔE_{disp} (equivalent to attractive forces due to instantaneous fluctuation of electron clouds in the fragment before and after bond formation) is also obtained as we used D3(BJ). The orbital term, ΔE_{orb} comes from (constructive interference during spatial mixing of orbitals of the fragments) the mixing of orbitals, charge transfer, and polarization between the isolated fragments. This can be further divided into contributions from each irreducible representation of the point group of an interacting system as follows:

$$\Delta E_{orb} = \sum_r \Delta E_r \quad (2)$$

The combined EDA-NOCV method is able to partition the total orbital interactions into pairwise contributions of the orbital interactions, which are important in providing a complete picture of the bonding. The charge deformation $\Delta\rho_k(r)$, which comes from the mixing of the orbital pairs $\psi_k(r)$ and $\psi_{-k}(r)$ of the interacting fragments, gives the magnitude and the shape of the charge flow due to the orbital interactions (eq 3), and the associated orbital energy, ΔE_{orb} presents the amount of orbital energy coming from such interaction (eq 4).

$$\Delta\rho_{orb}(r) - \sum_k \Delta\rho_k(r) = \sum_{k=1}^{N/2} v_k[-\psi^2{}_{-2}(r) + \psi^2{}_{-2}(r)] \quad (3)$$

$$\Delta E_{orb} = \sum_k \Delta E^k_{orb} = \sum_k \nu_k[-F^{TS}_{-k,-k} + F^{TS}_{k,k}] \quad (4)$$

Readers are further referred to the recent review articles to know more about the EDA-NOCV method and its application.[23] A thorough depiction of the EDA-NOCV approach and the meaning of each parameter is given in recent reviews/books.[9,16] Also, a very recent report related to eq 1 has been critically discussed by different researchers.[24]

RESULTS AND DISCUSSION

The optimized geometries of compounds $(L)C_5H_4$ (**1**−**3**) [L = H_2C (**1a**), aAAC (**1b**), $(CO_2Me)_2C$ (**1c**), Py (**1d**); aNHC (**2a**), NHC (**2b**), PPh_3 (**2c**); SNHC (**3**)] in singlet ground states are shown in Figure 1 and Scheme 3. The compounds were found to be stable in singlet states than in their triplet states by 28.1−55.1 kcal/mol (Figure S1). The C−C_L bond lengths in these compounds are in the range of 1.349−1.402 Å, which is close to the typical C═C bond length in ethylene (1.34 Å)/benzene (1.39 Å) and less than the sp^2−sp^2 carbon single bond distance (1.48 Å), suggesting a double bond character of the C−C_L bond.[8c,k] This C−C_L bond length varies

https://doi.org/10.1021/acsomega.1c00648
ACS Omega 2021, 6, 17798−17810

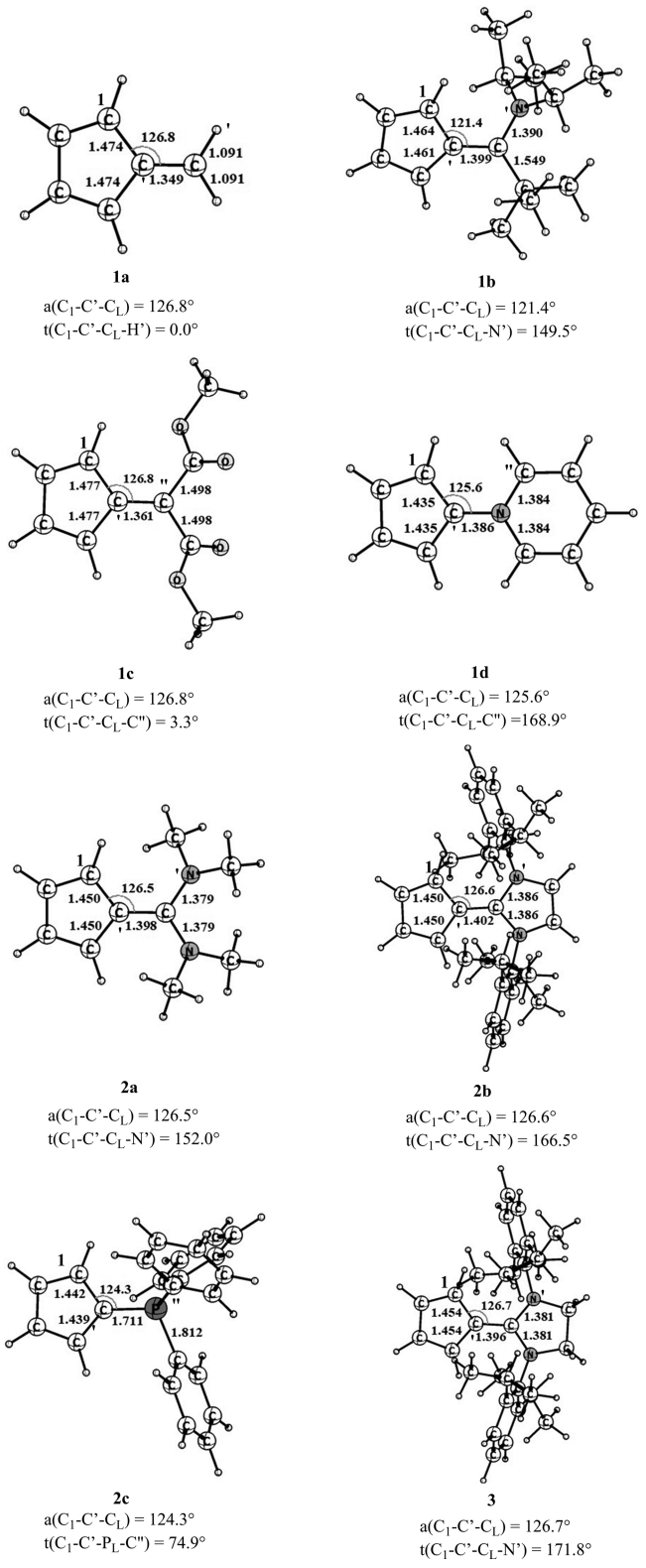

Figure 1. Optimized singlet state geometries of $(L)C_5H_4$ compounds (**1**–**3**) (L = CH_2, aAAC, $C(CO_2Me)_2$, pyridine, aNHC, NHC^{Dip}, PPh_3, $SNHC^{Dip}$) at the BP86-D3(BJ)/def2-TZVPP level of theory.

in the order **1a** < **1c** < **3** < **2a** < **1b** < **2b**. The increase in C–C_L bond distance is attributed to the steric crowding of the ligand or due to Pauli repulsion energy.[9] The C_{CP}–N bond length in **1d** (1.386 Å) is significantly longer than the C=N double bond of imine (1.279 Å) and close to C–N bond lengths in pyridine (1.35 Å), indicating a partial double bond character. Meanwhile, the C_{CP}–P bond length in **2c** (1.711 Å) is very close to the value (1.6993 (5) Å) reported for the ylide Ph_3P=CH–Ph,[25a] significantly shorter than the typical C–P single bond distance (1.81–1.84 Å) and close to the C–P partial double bond lengths (1.698–1.703 Å) in phosphinidenide anion.[25b] Geometrical parameters of the compounds **1a**, **1d**, **2a**, **2b**, and **2c**, calculated at the BP86-D3(BJ)/def2-T-ZVPP level correlated well with the experimental values reported by Mueller-Westerhoff,[8b] Kunz et.al,[8c] Ramirez et.al,[8a] and Lloyd et al.[26] The C_1–C′–C_L bond angles in compounds **1a** to **3** are in the range of 121.4–126.8°. The torsion angles show that the C_5H_4 unit and the ligand lie in the same plane in **1a** and **1c**, while they deviate from the plane in all other compounds.

The thermodynamic stability of L–C_5H_4 compounds has been assessed from the dissociation of L–C_5H_4 into C_5H_4 and L units (L = CH_2, aAAC, $C(CO_2Me)_2$, pyridine, aNHC, NHC^{Dip}, PPh_3, $SNHC^{Dip}$). The bond dissociation energy (BDE) values (Table S1) were calculated at 0 K and the change in Gibbs free energy at 298 K (ΔG^{298}). The D_e values of the compounds **1a** to **3** vary from 81.6 to 190 kcal/mol, depending on the ligand L. Among all the ligands, the CH_2 ligand in **1a** is strongly bound to C_5H_4 (D_e = 190 kcal/mol) followed by $C(CO_2Me)$ (D_e = 156.9 kcal/mol), while pyridine (D_e = 81.6 kcal/mol) is comparatively weakly bound followed by PPh_3 (D_e = 92.2 kcal/mol). The bond dissociation energies of carbene ligands (L = aAAC, aNHC, NHC, SNHC) lie in between, with SNHC having higher bond strength (D_e = 132.7 kcal/mol) followed by aAAC (D_e = 129.4 kcal/mol), aNHC (D_e = 128.3 kcal/mol), and NHC (D_e = 128.0 kcal/mol). In general, the bond energy of a coordinate/dative single bond is lower than that of an electron-sharing single bond.[12b−d]

The dissociation of L–C_5H_4 is significantly endergonic at room temperature with endergonicity (ΔG^{298}) values ranging from 64.9 to 171.7 kcal/mol. Substantially high dissociation energies and reasonably high endergonicity ascertain the thermodynamic stability of L–C_5H_4 compounds. Another stability parameter that indicates the electronic stability is the HOMO–LUMO energy gap ($\Delta_{H\text{-}L}$). High $\Delta_{H\text{-}L}$ denotes higher electronic stability and less reactivity. The L–C_5H_4 compounds exhibit a high HUMO–LUMO energy gap (40.1–63.5 kcal/mol) indicating their electronic stability.

We have employed various methods to analyze the bonding situation in L–C_5H_4 compounds, **1a** to **3** [L = H_2C (**1a**), aAAC (**1b**), $(CO_2Me)_2C$ (**1c**), Py (**1d**); aNHC (**2a**), NHC (**2b**), PPh_3 (**2c**); SNHC (**3**)]. The NBO results from Table 1 shows σ and π occupancies of 1.97–1.99 and 1.66–1.81 e, respectively for L–C_5H_4 bonds in almost all compounds except **1d** and **2c**, where only σ occupancies are prominent. The σ and π bonds are almost equally polarized with a slight inclination toward the C_5H_4 ring in compounds **1a**, **1b**, and **1c**, whereas in compounds **2a**, **2b**, and **3**, σ bonds are almost equally polarized and π bonds are more polarized toward the C_5H_4 ring. The C_{C5H4}–N_{Py} σ bond of **1d** is more polarized toward N. The C_{C5H4}–P_{PPh3} σ bond of **2c** is more polarized toward the C_5H_4 ring. NBO analysis shows an accumulation of charge on the C_5H_4 ring in all compounds except compound **1c**. The slightly positive charge on the C_5H_4 ring in **1c** is due to the electron-withdrawing effect of two CO_2Me groups in the ligand part. The Wiberg bond indices (WBI) values of 1.34–1.77 support the partial double bond character in all compounds except **1d** and **2c**. The WBI values of 1.07 (**1d**) and 1.14 (**2c**) indicate a very weak partial double bond

https://doi.org/10.1021/acsomega.1c00648
ACS Omega 2021, 6, 17798−17810

Scheme 3. Cyclopentadienyl-Carbene/Phosphene Compounds L−C_5H_4 (L = CH_2, aAAC, $C(CO_2Me)_2$, Pyridine, aNHC, NHC^{Dip}, PPh_3, $SNHC^{Dip}$) (1a-1d, 2a-2c, 3)[a]

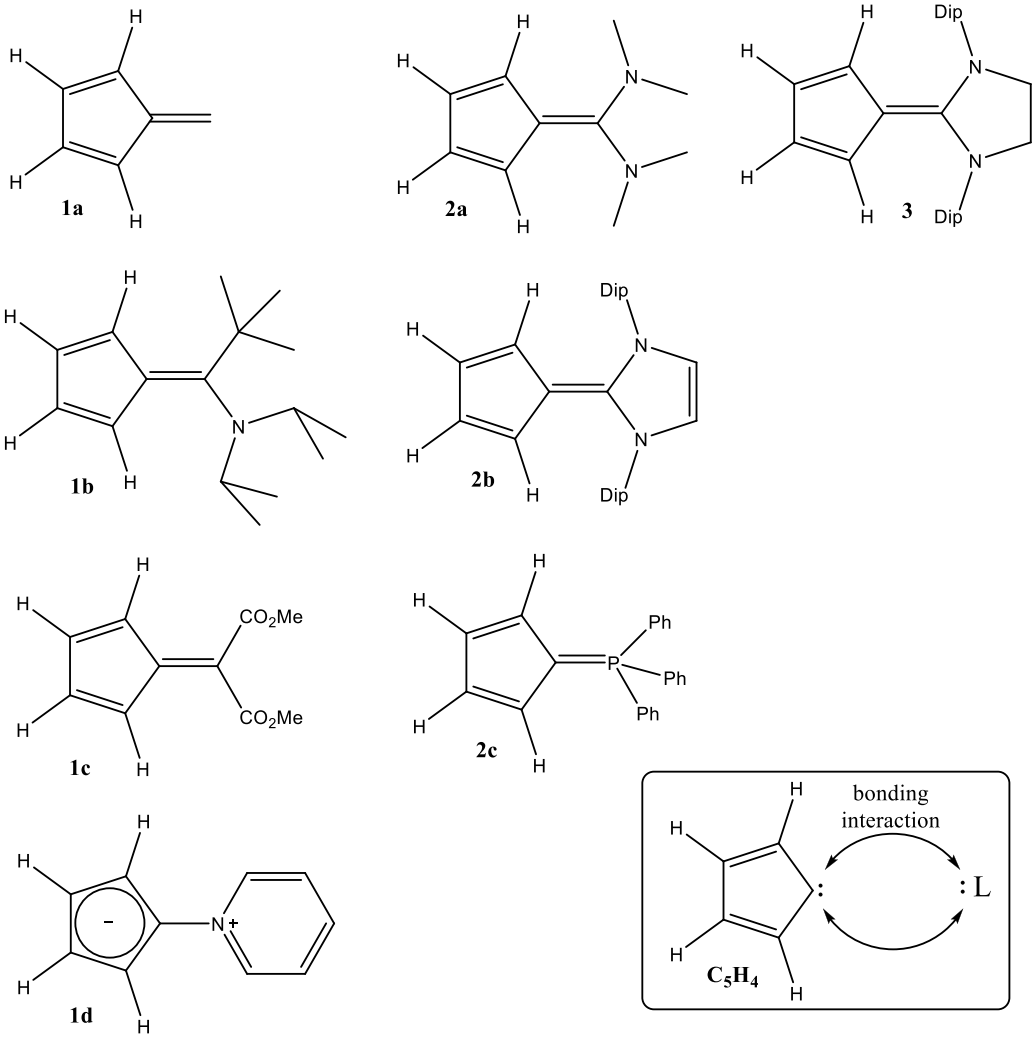

[a]See reference 8 for relevant previously reported compounds.

Table 1. NBO Results of the (L)C_5H_4 Compounds [L = H_2C (1a), aAAC (1b), $(CO_2Me)_2C$ (1c), Py (1d); aNHC (2a), NHC (2b), PPh_3 (2c); SNHC (3)] at the BP86/def2-TZVPP Level of Theory[a]

compound	bond	ON	L-C_1 polarization and hybridization (%)		WBI	q (C_5H_4)
1a	C_L−C_1 σ	1.99	C_L: 48.1 s(39.9), p(60.1)	C_{Cp}: 51.9 s(38.3), p(61.7)	1.77	−0.126
	C_L−C_1 π	1.81	C_L: 48.1 s(0.3), p(99.7)	C_{Cp}: 51.9 s(0.5), p(99.5)		
1b	C_L−C_1 σ	1.97	C_L: 49.1 s(37.2), p(62.8)	C_{Cp}: 50.9 s(36.8), p(63.2)	1.46	−0.371
	C_L−C_1 π	1.69	C_L: 43.6 s(0.2), p(99.8)	C_{Cp}: 56.4 s(0.1), p(99.9)		
1c	C_L−C_1 σ	1.98	C_L: 50.5 s(41.0), p(59.0)	C_{Cp}: 49.5 s(36.9), p(63.1)	1.64	0.021
	C_L−C_1 π	1.75	C_L: 51.5 s(0.1), p(99.9)	C_{Cp}: 48.5 s(0.1), p(99.9)		
1d	C_L−N σ	1.98	N: 63.5 s(35.4), p(64.6)	C_{Cp}: 36.5 s(29.1), p(70.9	1.14	−0.238
2a	C_L−C_1 σ	1.97	C_L: 50.7 s(40.1), p(59.9)	C_{CP}: 49.3 s(34.4), p(65.6)	1.34	−0.470
	C_L−C_1 π	1.66	C_L: 41.7 s(0.1), p(99.9)	C_{Cp}: 58.3 s(0.1), p(99.9)		
2b	C_L−C_1 σ	1.97	C_L: 50.7 s(40.1), p(59.9)	C_{Cp}: 49.3 s(34.4), p(65.6)	1.34	−0.470
	C_L−C_1 π	1.66	C_L: 41.7 s(0.1), p(99.9)	C_{Cp}: 58.3 s(0.1), p(99.9)		
2c	C_L−P σ	1.97	P: 41.6 s(30.5), p(69.5)	C_{Cp}: 58.4 s(31.0), p(69.0)	1.07	−0.915
3	C_L−C_1 σ	1.97	C_L: 50.9 s(41.9), p(58.1)	C_{Cp}: 49.1 s(34.7), p(65.3)	1.35	−0.472
	C_L−C_1 π	1.67	C_L: 40.7 s(0.1), p(99.9)	C_{Cp}: 59.3 s(0.1), p(99.9)		

[a]Occupation number, ON, polarization and hybridization of the L−C_5H_4 bonds, and partial charges, q.

character in **1d** and **2c**. These compounds[8a−c] are reported to be very polar (dipole moment >7 D).[8c] The HOMO of almost all compounds is mainly the π* MOs of the C_5H_4 ring, while HOMO-1 indicates L−C_{Cp} π interactions except for compound **1d**, where the HOMO indicates L−C_{C5H4} π interactions and HOMO-1 represents the π* MO of the

https://doi.org/10.1021/acsomega.1c00648
ACS Omega 2021, 6, 17798−17810

Table 2. QTAIM Results of the (L)C_5H_4 Compounds [L = H_2C (1a), aAAC (1b), $(CO_2Me)_2C$ (1c), Py (1d); aNHC (2a), NHC (2b), PPh_3 (2c); SNHC (3)]

molecule	bonds	$\rho(r)$	$\nabla^2\rho(r)$	$H(r)$	$V(r)$	$G(r)$	ε	η
1a	C_L-C_{Cp}	0.342	−1.025	−0.388	−0.518	0.130	0.255	2.253
1b	C_L-C_{Cp}	0.309	−0.863	−0.324	−0.433	0.109	0.252	1.961
1c	C_L-C_{Cp}	0.332	−0.967	−0.369	−0.495	0.126	0.254	2.158
1d	N-C_{Cp}	0.291	−0.670	−0.635	−0.702	0.267	0.265	1.412
2a	C_L-C_{Cp}	0.310	−0.878	−0.331	−0.442	0.111	0.261	2.042
2b	C_L-C_{Cp}	0.302	−0.846	−0.326	−0.441	0.114	0.249	2.077
2c	P-C_{Cp}	0.193	−0.088	−0.193	−0.365	0.171	0.229	0.664
3	C_L-C_{Cp}	0.307	−0.871	−0.334	−0.451	0.116	0.262	2.102

Scheme 4. Bonding Possibilities of L−C_5H_4 Compounds (L = CH_2, aAAC, $C(CO_2Me)_2$, Pyridine, aNHC, NHC^{Dip}, PPh_3, $SNHC^{Dip}$) (1a-d, 2a-c, 3)

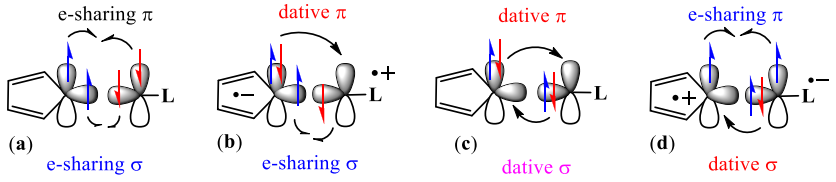

Table 3. EDA-NOCV Results of L-C_5H_4 Bonds of (L)C_5H_4 Compounds (L = CH_2, aAAC, $C(CO_2Me)_2$, Pyridine, aNHC, NHC^{Dip}, PPh_3, $SNHC^{Dip}$) Using Four Different Sets of Fragments with Different Charges and Electronic States (S = Singlet, D = Doublet, T = Triplet) and Associated Bond Types at the BP86-D3(BJ)/TZ2P Level[b]

Molecule	Bond type[a]	Fragments	ΔE_{int}	ΔE_{Pauli}	ΔE_{elstat}	ΔE_{disp}	ΔE_{orb}
1a	D	CH_2 (S) + Cp (S)	-285.1	295.6	-188.9	-2.7	-389.2
	E	CH_2 (T) + Cp (T)	-181.5	305.8	-192.6	-2.7	**-291.9**
	D+E σ-Sharing	$[CH_2]^+$ (D) + $[Cp]^-$ (D)	-388.9	318.5	-298.8	-2.7	-405.9
	D + E π-Sharing	$[CH_2]^+$ (D) + $[Cp]^-$ (D)	-433.0	365.3	-349.1	-2.7	-446.5
1b	D	aAAC (S) + Cp (S)	-197.2	365.9	-212.2	-11.3	-339.7
	E	aAAC (T) + Cp (T)	-175.1	412.9	-247.3	-11.3	**-329.3**
	D+E σ-Sharing	$[aAAC]^+$ (D) + $[Cp]^-$ (D)	-262.3	438.4	-324.0	-11.3	-365.4
	D + E π-Sharing	$[aAAC]^+$ (D) + $[Cp]^-$ (D)	-319.7	592.3	-411.1	-11.3	-489.7
1c	D	$(CO_2Me)_2C$ (S) + Cp (S)	-417.4	334.5	-183.4	-6.8	-561.6
	E	$(CO_2Me)_2C$ (T) + Cp (T)	-172.0	384.8	-218.3	-6.8	**-331.8**
	D+E σ-Sharing	$[(CO_2Me)_2C]^+$ (D) + $[Cp]^-$ (D)	-343.8	435.6	-322.3	-6.8	-450.2
	D + E π-Sharing	$[(CO_2Me)_2C]^+$ (D) + $[Cp]^-$ (D)	-363.8	571.0	-413.2	-6.8	-514.7
1d	D	Py (S) + Cp (S)	-326.2	278.8	-183.2	-5.6	-416.2
	E	Py (T) + Cp (T)	-175.8	417.8	-219.0	-5.6	**-369.0**
	D+E σ-Sharing	$[Py]^+$ (D) + $[Cp]^-$ (D)	-260.7	449.7	-306.8	-5.6	-398.0
	D + E π-Sharing	$[Py]^+$ (D) + $[Cp]^-$ (D)	-899.2	690.3	-362.8	-5.6	-1221.1
2a	D	aNHC (S) + Cp (S)	-386.0	339.4	-247.9	-8.3	-469.2
	E	aNHC (T) + Cp (T)	-299.8	406.8	-265.0	-8.3	-433.3
	D+E σ-Sharing	$[aNHC]^+$ (D) + $[Cp]^-$ (D)	-249.2	450.2	-338.1	-8.3	**-352.1**
	D + E π-Sharing	$[aNHC]^+$ (D) + $[Cp]^-$ (D)	-325.7	567.8	-408.4	-8.3	-476.8
2b	D	NHC (S) + Cp (S)	-379.4	318.3	-225.9	-16.5	-455.3
	E	NHC (T) + Cp (T)	-404.1	440.8	-266.1	-16.5	-562.4
	D+E σ-Sharing	$[NHC]^+$ (D) + $[Cp]^-$ (D)	-293.1	464.3	-326.9	-16.5	**-414.0**
	D + E π-Sharing	$[NHC]^+$ (D) + $[Cp]^-$ (D)	-406.2	711.0	-456.2	-16.5	-644.5
2c	D	PPh_3 (S) + Cp (S)	-391.4	262.8	-495.7	-12.3	-495.7
	E	PPh_3 (T) + Cp (T)	-337.4	362.9	-220.1	-12.3	-467.8
	D+E σ-Sharing	$[PPh_3]^+$ (D) + $[Cp]^-$ (D)	-263.7	375.5	-298.6	-12.3	**-328.2**
	D + E π-Sharing	$[PPh_3]^+$ (D) + $[Cp]^-$ (D)	-787.1	582..6	-312.1	-12.3	-1045.3
3	D	SNHC (S) + Cp (S)	-182.3	367.7	-209.9	-20.0	**-320.1**
	E	SNHC (T) + Cp (T)	-224.8	412.9	-238.7	-20.0	-379.1
	D+E σ-Sharing	$[SNHC]^+$ (D) + $[Cp]^-$ (D)	-261.5	512.3	-341.8	-20.0	-412.0
	D + E π-Sharing	$[SNHC]^+$ (D) + $[Cp]^-$ (D)	-368.1	691.9	-435.6	-20.0	-604.4

[a]D = dative bond; E = electron-sharing bond. [b]Energies are in kcal/mol. The most favorable fragmentation scheme and bond type are given by the smallest ΔE_{orb} value written in red.

C_5H_4 ring (Figure S2). The quantum theory of atoms in molecules (QTAIM) calculations have been carried out to further explore the bonding pattern in L−C_5H_4 compounds. The results from Table 2 shows the ellipticity values of 0.229−

https://doi.org/10.1021/acsomega.1c00648
ACS Omega 2021, 6, 17798−17810

Scheme 5. The Best Bonding Scenarios of $(L)C_5H_4$ Compounds 1a−b, 2a−c, 3 (L = H_2C, aAAC; $(CO_2Me)_2C$, Py; aNHC, NHC^{Dip}, PPh_3; $SNHC^{Dip}$) at the BP86-D3(BJ)/TZ2P Level of Theory

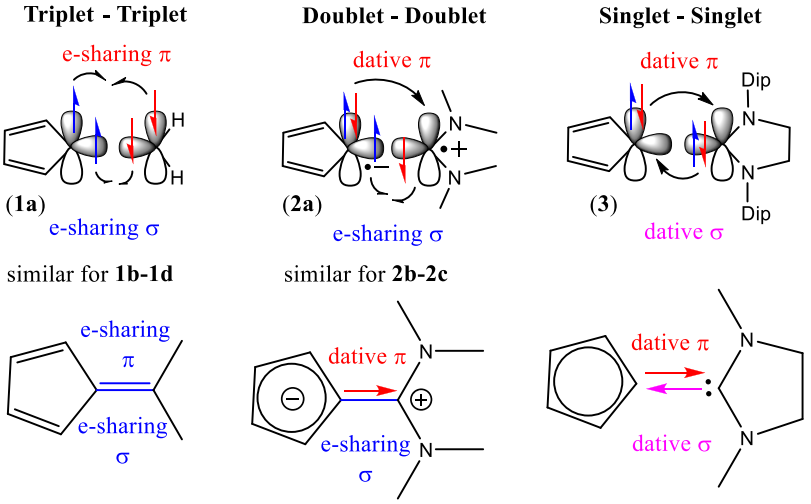

[a]The arrow represents covalent dative bond.

0.265 for L−C_5H_4 bond in compounds **1a** to **3**. The ellipticity ($\varepsilon_{BCP} = \lambda_1/\lambda_2 - 1$) is a measure of the bond order, and in general, the ε_{BCP} of a single and triple bond is close to zero because of the cylindrical contours of electron density, ρ, while for a double bond, the value is greater than zero.[27] This is due to the asymmetric distribution of electron density, ρ perpendicular to the bond path for a double bond. The ellipticity values of current compounds under study are deviated from the cylindrical contours, indicating the double bond character with reasonable π contribution, and are in good agreement with WBI values. The (3, −1) bond critical points (BCPs) of the L−C_5H_4 bond in compounds **1a** to **3** are characterized with reasonably high negative Laplacian $\nabla^2\rho(r)$ and total energy density $H(r)$ along with considerable local electron densities $\rho(r)$ of 0.193−0.342 a.u., indicating open-shell interactions. The disparity in electron density, ρ(r) and total energy density, $H(r)$ in all compounds except **1d** and **2c** can be attributed to C−C_L bond lengths. The local electron density, $\rho(r)$ and total energy density, $H(r)$ at the BCP (Table2) decrease with an increase in C−C_L bond length (Figure 1). Thus, the compounds with shorter C−C_L bond length shows higher electron density, $\rho(r)$ and total energy density, $H(r)$. The Laplacian of electron density contour plots shows that the BCPs (green dots) are located at the center of the bond path for compounds **1a**, **1b**, and **1c**, whereas it is slightly polarized toward the C_5H_4 ring in compounds **2a**, **2b**, and **3**. In **1d**, the BCP is polarized toward the C_5H_4 ring, and in **2c**, it is polarized toward the P atom (Figure S3). The ε_{BCP} value (0.229) of **2c** is significantly lower than that of the reported ylide $Ph_3P{=}CH{-}Ph$ (0.510).[25a] The η value determines the covalency of the bond: an η value greater than 1.0 indicates the covalent nature of the bond and a value less than 1.0 indicates a closed-shell nature. The η values of 1.413−2.253 suggest that the L−C_5H_4 bond is more covalent in compounds **1a** to **3**. The AIM analysis of the current systems under study shows a reasonably high negative Laplacian of electron density and a lowering in potential energy, which supports covalent bonding and rules out the possibility of charge shift bonding.

It should be noted that NBO and QTAIM methods cannot distinguish the dative or electron sharing interactions and hence the classification of L−C_5H_4 bonds as dative or electron sharing remains elusive. In this regard, the acumen of energy decomposition analysis−natural orbitals for chemical valence (EDA−NOCV) is helpful to give a detailed insight into the nature of the chemical bonds of L−C_5H_4 compounds [L = H_2C (**1a**), aAAC (**1b**), $(CO_2Me)_2C$ (**1c**), Py (**1d**); aNHC (**2a**), NHC (**2b**), PPh_3 (**2c**); SNHC (**3**)] by its ability to provide the best bonding model to represent the overall bonding situation in the molecule. The bonding model with the lowest ΔE_{orb} is contemplated as the best bonding representation since it needs the least change in the electronic charge of the fragments to make the electronic structure of the compound.[28]

We have considered four different bonding possibilities (Scheme 4) by varying the electronic states of interacting fragments L and C_5H_4, to give the best description of the L−C_5H_4 bonds in the compounds **1a** to **3** [L = H_2C (**1a**), aAAC (**1b**), $(CO_2Me)_2C$ (**1c**), Py (**1d**); aNHC (**2a**), NHC (**2b**), PPh_3 (**2c**); SNHC (**3**)]. These are (a) neutral L and C_5H_4 fragments in their electronic triplet states forming electron-sharing σ and π bonds, (b) singly charged $[L]^+$ and $[C_5H_4]^-$ fragments in their electronic doublet states, which would interact to form electron-sharing σ and dative π bonds, (c) neutral L and C_5H_4 fragments in their electronic singlet states forming both σ and π dative bonds, and finally (d) singly charged $[L]^+$ and $[C_5H_4]^-$ fragments in their electronic doublet states interacting to form σ dative and π electron-sharing bonds. Table 3 shows the numerical results of all possible bonding situations with different fragmentation modes. Based on the lowest ΔE_{orb} value, compounds **1a** to **3** can be categorized with three different bonding patterns. Compounds **1a** to **1d** prefer to form electron-sharing σ and π bonds (L=C_5H_4) resulting from the interaction of neutral L and C_5H_4 fragments in their electronic triplet, whereas compounds **2a** to **2c** choose to form electron-sharing σ (L−C_5H_4) and dative π (L ← C_5H_4) bonds with the interaction of $[L]^+$ and $[C_5H_4]^-$fragments in their electronic doublet states. In contrast, compound **3** prefers to form dative σ (L → C_5H_4) and dative π bonds (L ← C_5H_4) with the interaction of neutral L and C_5H_4 fragments in their electronic singlet states (Scheme 5). Dative bonds are represented with arrows (→)

https://doi.org/10.1021/acsomega.1c00648
ACS Omega 2021, 6, 17798−17810

Table 4. EDA-NOCV Results at the BP86-D3(BJ)/TZ2P Level of L-C_5H_4 Bonds of (L)C_5H_4 Compounds (L = CH_2 (1a) aAAC (1b), $C(CO_2Me)_2$ (1c) Py (1d)) Compounds Using Neutral L and Cp in the Electronic Triplet (T) States as Interacting Fragments[c]

energy	interaction[c]	CH_2 (T) + C_5H_4 (T) **1a**	aAAC (T) + C_5H_4 (T) **1b**	$C(CO_2Me)_2$ (T) + C_5H_4 (T) **1c**	Py (T) + C_5H_4 (T) **1d**
ΔE_{int}		−181.5	−175.1	−172.0	−175.8
ΔE_{Pauli}		305.8	412.9	384.8	417.8
ΔE_{disp}[a]		−2.7 (0.5%)	−11.3 (2%)	−6.8 (1.2%)	−5.6 (1%)
ΔE_{elstat}[a]		−192.6 (39.5%)	−247.3 (42%)	−218.3 (39.2%)	−219.0 (36.9%)
ΔE_{orb}[a]		−291.9 (60%)	−329.3 (56%)	−331.8 (59.6%)	−369.0 (62.1%)
$\Delta E_{orb(1)}$[b]	L-C_5H_4 σ e^- sharing	−207.6 (71.1%)	−200.3 (60.8%)	−230.6 (69.5%)	−275.3 (74.6%)
$\Delta E_{orb(2)}$[b]	L-C_5H_4 π e^- sharing	−66.2 (22.6%)	−93.0 (28.2%)	−68.7 (20.7%)	−53.5 (14.5%)
$\Delta E_{orb(3)}$[b]	L ← C_5H_4 π back donation	−7.7 (2.6%)			
	L-C_5H_4 σ polarization		−18.8 (5.7%)	−15.9 (4.8%)	−18.8 (5.1%)
$\Delta E_{orb(4)}$[b]	L ← C_5H_4 σ back donation	−4.2 (1.4%)			
	L ← C_5H_4 π back donation		−8.2 (2.5%)	−10.2 (3.1%)	−8.7 (2.3%)
$\Delta E_{orb(5)}$[b]	L → C_5H_4 π donation				−6.6 (1.8%)
$\Delta E_{orb(rest)}$[b]		−6.2 (2.1%)	−9.0 (2.7%)	−6.4 (1.9%)	−6.1 (1.6%)

[a]The values in parentheses show the contribution to the total attractive interaction $\Delta E_{elstat} + \Delta E_{orb} + \Delta E_{disp}$. [b]The values in parentheses show the contribution to the total orbital interaction ΔE_{orb}. [c]Energies are in kcal/mol.

Table 5. EDA-NOCV Results at the BP86-D3(BJ)/TZ2P Level of L-C_5H_4 Bonds of (L)C_5H_4 Compounds (L = aNHC (2a), NHC^{Dip} (2b) PPh_3 (2c), $SNHC^{Dip}$ (3)) Using Singly Charged $[L]^+$ and $[C_5H_4]^-$ in the Electronic Doublet (D) States as Interacting Fragments for L = aNHC, NHC^{Dip}, PPh_3 and Neutral L and C_5H_4 in the Electronic Singlet (T) States as Interacting Fragments for L = $SNHC^{Dip}$[c]

Energy	Interaction[c]	$[aNHC]^+$ (D) + $[C_5H_4]^-$ (D) **2a**	$[NHC]^+$ (D) + $[C_5H_4]^-$ (D) **2b**	$[PPh_3]^+$ (D) + $[C_5H_4]^-$ (D) **2c**	SNHC (S) + C_5H_4 (S) **3**
ΔE_{int}		−249.2	−293.1	−263.7	−182.3
ΔE_{Pauli}		450.2	464.3	375.5	367.7
ΔE_{disp}[a]		−8.2 (1.2%)	−16.5 (2.2%)	−12.3 (2%)	−20.0 (3.6%)
ΔE_{elstat}[a]		−338.1 (48.4%)	−326.9 (43.1%)	−298.6 (46.7%)	−209.9 (38.2%)
ΔE_{orb}[a]		−352.1 (50.4%)	−414.3 (54.7%)	−328.2 (51.3%)	−320.1 (58.2%)
$\Delta E_{orb(1)}$[b]	L-C_5H_4 σ e^- sharing	−248.9 (70.7%)	−265.8 (64.1%)	−197.2 (60%)	
	L → C_5H_4 σ donation				−243.1 (76.0%)
$\Delta E_{orb(2)}$[b]	L ← C_5H_4 π back donation	−62.4 (17.7%)	−69.5 (16.7%)	−54.0 (16.4%)	−43.8 (13.7%)
$\Delta E_{orb(3)}$[b]	L → C_5H_4 σ donation	−21.2 (6.0%)	−33.4 (8.0%)		
	L ← C_5H_4 σ back donation			−18.9 (5.6%)	−11.9 (3.7%)
$\Delta E_{orb(4)}$[b]	L ← C_5H_4 π back donation	−9.2 (2.6%)	−17.4 (4.2%)	15.0 (4.6%)	
$\Delta E_{orb(5)}$[b]	C_5H_4 π polarization		−5.4 (1.3%)	−11.4 (3.5%)	
$\Delta E_{orb(6)}$[b]	C_5H_4 π polarization			−5.8 (1.7%)	
$\Delta E_{orb(rest)}$[b]		−10.4 (3.0%)	−22.8 (5.5%)	−25.9 (7.9%)	−21.3 (6.6%)

[a]The values in parentheses show the contribution to the total attractive interaction $\Delta E_{elstat} + \Delta E_{orb} + \Delta E_{disp}$. [b]The values in parentheses show the contribution to the total orbital interaction ΔE_{orb}. [c]Energies are in kcal/mol.

according to the DCD model,[29] and this helps in distinguishing dative bonds from electron-sharing bonds.[12]

The detailed EDA-NOCV results of the most appropriate bonding possibility showing pairwise orbital interactions are given in Tables 4 and 5. The intrinsic interaction energy (ΔE_{int}) denotes the overall strength of the bond, and ΔE_{int} values of the eight compounds vary in the order of **1c** < **1b** < **1d** < **1a** < **3** < **2a** < **2c** < **2b**. The intrinsic strength, ΔE_{int} values of almost all compounds except compound **1a** are significantly larger than the bond dissociation energies, which might be due to the larger preparative energies (ΔE_{prep}) of the fragments. The preparative energies originate from the changes in the geometry of the fragments from their equilibrium structure to the geometry in the compound and from the electronic excitation to a reference state. The high intrinsic interaction energies of compounds despite large Pauli repulsion energies can be attributed to the high orbital and electrostatic contributions. The total orbital (covalent) interactions (ΔE_{orb}) contribute 50.4−62.1% to the total attractive interactions. This is in accord with the negative Laplacian and total energy densities of QTAIM calculations. The remaining contributions come from electrostatic (36.9−48.4%) and dispersion (0.5−3.6%) interactions. The electrostatic contribution is higher in compounds **2a** to **3** compared to compounds **1a** to **1d**. The breakdown of ΔE_{orb} into pairwise contributions further sheds light on the strength and type of interactions. The deformation densities and associated molecular orbitals as shown in Figures 2 and 3 and Figures S4−S8 help in visualizing the direction of charge flow and shape of interacting MOs of the ligands and C_5H_4 fragments.

The results from Table 4 illustrates four pairwise contributions for compounds **1a** to **1c** and five pairwise interactions for compound **1d** (Figure 2, Figures S4−S6). The strongest orbital interaction, $\Delta E_{orb(1)}$ arise from the electron sharing σ interactions between unpaired electrons in the SOMO of the fragments and contributes 60.8−74.6% of total orbital interactions. $\Delta E_{orb(2)}$ represents the electron-sharing π interactions between unpaired electrons in the SOMO of the

https://doi.org/10.1021/acsomega.1c00648
ACS Omega 2021, 6, 17798−17810

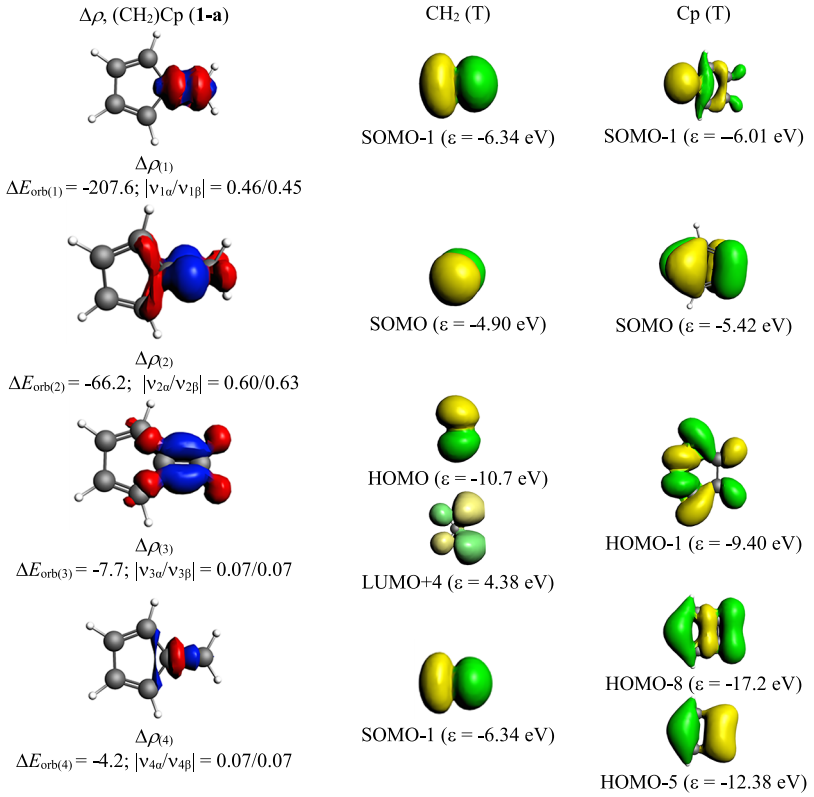

Figure 2. Shape of the deformation densities, $\Delta\rho_{(1)-(4)}$ that correspond to $\Delta E_{orb(1)-(4)}$, and the associated MOs of $CH_2-C_5H_4$ (**1a**) and the fragment orbitals of CH_2 and C_5H_4 in the triplet state at the BP86-D3(BJ)/TZ2P level. Isosurface values are 0.003 a.u. for $\Delta\rho_{(1)-(4)}$. The eigenvalues, $|\nu_n|$ give the size of the charge migration in e. The direction of the charge flow of the deformation densities is red → blue.

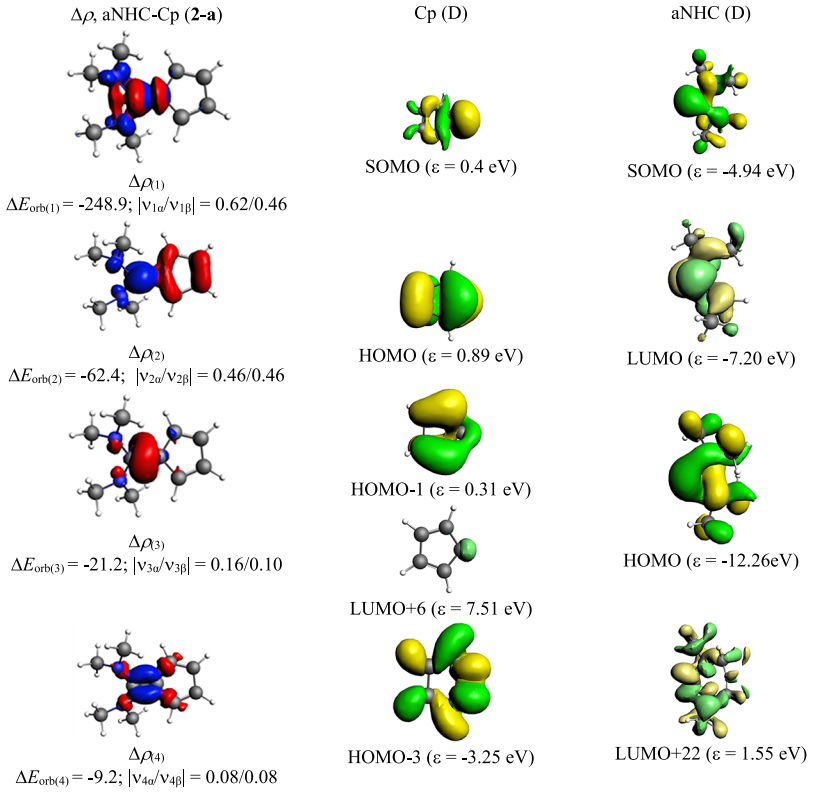

Figure 3. Shape of the deformation densities, $\Delta\rho_{(1)-(4)}$ that correspond to $\Delta E_{orb(1)-(4)}$, and the associated MOs of aNHC-C_5H_4 (**2a**) and the fragment orbitals of aNHC and C_5H_4 in the triplet state at the BP86-D3(BJ)/TZ2P level. Isosurface values are 0.003 a.u. for $\Delta\rho_{(1)-(4)}$. The eigenvalues, $|\nu_n|$ give the size of the charge migration in e. The direction of the charge flow of the deformation densities is red → blue.

https://doi.org/10.1021/acsomega.1c00648
ACS Omega 2021, 6, 17798−17810

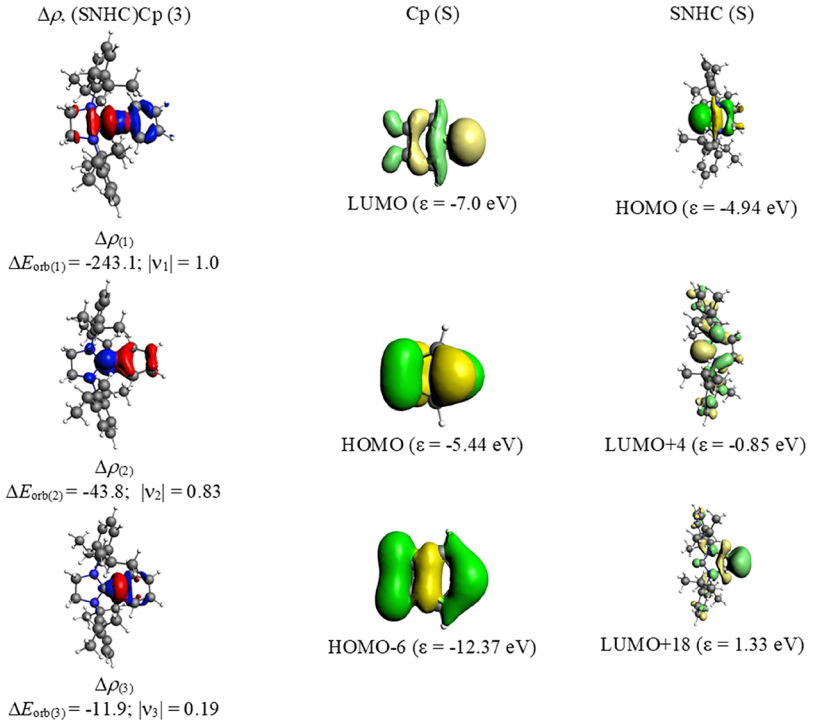

Figure 4. Shape of the deformation densities $\Delta\rho_{(1)-(3)}$ that correspond to $\Delta E_{orb(1)-(3)}$, and the associated MOs of SNHC- C_5H_4 (**3**) and the fragment orbitals of SNHC and C_5H_4 in the triplet state at the BP86-D3(BJ)/TZ2P level. Isosurface values are 0.003 a.u. for $\Delta\rho_{(1)-(3)}$. The eigenvalues, $|\nu_n|$ give the size of the charge migration in e. The direction of the charge flow of the deformation densities is red → blue.

fragments and contributes 14.5−28.2% of the total orbital interactions. There are other weak π interactions and $\Delta E_{orb(5)}$ in **1d** coming from the π back donation from filled orbitals of C_5H_4 into vacant orbitals of ligands (L ← C_5H_4) as represented by $\Delta E_{orb(3)}$ in **1a**, $\Delta E_{orb(4)}$ in **1b** to **1d**, and π donation from the ligand to C_5H_4 (L → C_5H_4). These weak π interactions provide 2.5−3.1% to the total orbital interactions. Collectively, the relative strength of π interactions is much smaller than the σ interactions. The strength of π interactions of compounds **1a** to **1d** varies in the order of ligand as pyridine (**1d**) < $C(CO_2Me)_2$ (**1c**) < CH_2 (**1a**) < aAAC (**1b**) according to the π accepting ability of the ligand. $\Delta E_{orb\ (3)}$ represents σ polarization in compounds **1b** to **1d** and contributes 4.8 to 5.7% to the total orbital interactions. The detailed EDA-NOCV analysis of pyridine analogues (**1d**) shows that the bonding scenario is not as simple as it shows in its structure. Pyridine units like to form a bond with C_5H_4 units in **1d** when both fragments are in triplet states. The π-bonding overlap between Py and C_5H_4 units is very weak. This π bond might be due to the dipolar interactions between one unpaired electron in each unit with opposite spins.

Table 5 shows the detailed EDA-NOCV results of compounds **2a** to **2c**, which prefers to form electron-sharing σ and dative π bonds, and compound **3**, which prefers both σ and π dative bonds. The results indicate four pairwise interactions for compounds **2a** and **3**, five pairwise interactions for **2b**, and six pairwise interactions for **2c** (Figure 3, Figures S7 and S8). In compounds **2a** to **2c**, the strongest interaction, $\Delta E_{orb\ (1)}$ providing 60−70.7% to the total orbital interactions comes from the electron-sharing σ interaction. The weaker $\Delta E_{orb(2)}$ (16.4−17.7%) and $\Delta E_{orb(4)}$ (2.6−4.6%) are due to π back donation (L ← C_5H_4) from filled HOMO, HOMO-1, and HOMO-3 to the vacant LUMO and high lying LUMOs of ligands L (L = aNHC (**2a**), NHC (**2b**), PPh_3 (**2c**)), respectively. The relative contribution due to electron-sharing σ interactions is much higher than the π interactions. The dative π interactions of compounds **2a** to **2c** are weaker compared to those of **1a** to **1d**. $\Delta E_{orb(3)}$ (5.6−8%) represents ligand (aNHC (**2a**), NHC (**2b**)) to C_5H_4 σ donation (L → C_5H_4) from the HOMO and HOMO-1 of ligands to LUMO +6 of C_5H_4 in compounds **2a** and **2b**, whereas in compound **2c**, it represents C_5H_4 to ligand (L) σ back donation (L ← C_5H_4) from the SOMO to LUMO+7 of ligand PPh_3. The other weak $\Delta E_{orb(5)}$ (1.3−3.5%) in compounds **2b** and **2c** and $\Delta E_{orb(6)}$ (1.7%) in compound **2c** are due to π polarizations. The $\Delta E_{orb\ (1)}$ of compound **3** arise from the σ donation (L → C_5H_4) from the HOMO of ligand (SNHC) to LUMO of C_5H_4 and contributes 76% to the total orbital interactions. The $\Delta E_{orb(2)}$ (13.7%) and $\Delta E_{orb(3)}$ (3.7%) come from the weak π back donation and σ back donation from C_5H_4 to ligand SNHC (L ← C_5H_4), respectively (Figure 4). Compound **1d** and **2c** are completely different from the bonding point of view.

We have calculated magnetic nucleus-independent chemical shifts (NICS), introduced by Schleyer et al.,[30] to measure the aromaticity of the five-membered Cp ring in L−C_5H_4 compounds (**1**−**3**) using the gauge-independent atomic orbital (GIAO) approach at the BP86/def2-TZVPP level on the geometries optimized at the BP86-D3(BJ)/def2-TZVPP level. The NICS method qualitatively and quantitatively describes the aromaticity, antiaromaticity, and nonaromaticity of ring systems and is considered as the most authentic probe of aromaticity due to its efficacy. NICS values calculated at the geometric centers of the ring are termed as NICS(0) and the values calculated at 1 Å above the plane of the ring are designated as NICS(1) (Table 6). Negative NICS values indicate aromaticity, and positive NICS values denote antiaromaticity, while values close to zero represent non-

https://doi.org/10.1021/acsomega.1c00648
ACS Omega 2021, 6, 17798−17810

Table 6. NICS Results of L-C_5H_4 Compounds at the BP86/def2-TZVPP Level

compound	NICS(0)	NICS(1)
1a	+1.518	−2.033
1b	−4.087	−5.940
1c	+4.157	+0.345
1d	−0.670	−2.770
2a	−6.101	−6.351
2b	−8.201	−7.639
2c	−8.877	−8.076
3	−7.638	−7.585

aromaticity. NICS(0) is considered as a measure of $\sigma + \pi$-electron delocalization and NICS(1) represents π-electron delocalization.[31] The positive NICS(0) and negative NICS(1) values of compound **1a** indicate the σ antiaromaticity and π aromaticity of the C_5H_4 ring. The positive NICS(0) and NICS(1) values of compound **1c** denotes σ and π antiaromaticity of the C_5H_4 ring. This is due to the electron-withdrawing effect of carboxyl groups of the ligand. The negative NICS(0) and NICS(1) values in all other compounds (**1b**, **1d**, **2a**, **2b**, **2c**, and **3**) indicates high σ and π aromaticity of the C_5H_4 ring in these systems and the aromaticity varies in the order **1d** < **1b** < **2a** < **3** < **2b** < **2c**. Compound **2c** shows high aromaticity, while compound **1d** shows the least aromaticity among all compounds although **1d** possesses a very high dipole moment.[8b,c]

SUMMARY AND CONCLUSIONS

In this work, we report the quantum chemical calculations of eight experimentally reported and not yet modeled L-C_5H_4 compounds (L = CH_2, aAAC, $C(CO_2Me)_2$, pyridine, aNHC, NHC^{Dip}, PPh_3, $SNHC^{Dip}$). The calculations suggest singlet ground-state geometries with reasonably high thermodynamic and electronic stabilities. The bonding analysis of L-C_5H_4 bonds by NBO, QTAIM, and EDA-NOCV methods nicely complement each other. EDA-NOCV calculations predict three different best bonding patterns under which the eight L-C_5H_4 compounds can be categorized. Compounds **1a** to **1d** prefer to form electron-sharing (L-C_5H_4) σ and π bonds with the interaction between L and C_5H_4 fragments in their electronic triplet states. Meanwhile, compounds **2a** to **2c** favors electron-sharing σ (L−Cp) and dative π bonds (L → C_5H_4) with the interaction of singly charged $[L]^+$ and $[C_5H_4]^-$ fragments in an electronic doublet state. On the other hand, compound **3** chooses to form dative σ (L → C_5H_4) and dative π bonds (L ← C_5H_4) with the interaction of neutral L and C_5H_4 fragments in their electronic singlet states. The calculated NICS values suggest the σ and π aromatic character of the C_5H_4 ring for almost all compounds except **1a** and **1c**. The computed values suggest σ antiaromaticity and π aromaticity of the C_5H_4 ring for **1a** and σ and π antiaromaticity of C_5H_4 the ring for **1c**. Overall, the detailed theoretical analysis of the current study throws light on the bonding and aromaticity of otherwise some of the well-known ligand-stabilized C_5H_4 ring compounds.

ASSOCIATED CONTENT

Supporting Information

The Supporting Information is available free of charge at https://pubs.acs.org/doi/10.1021/acsomega.1c00648.

Tables of dissociation energy (D_e), change in Gibbs free energy (ΔG^{298}), HOMO−LUMO gap ($\Delta_{H\text{-}L}$), and aromaticity of L−C_5H_4 complexes; tables of the optimized coordinates of **1a**−**d** singlet and triplet, **2a**−**c** singlet and triplet, and **3** singlet and triplet; figures of the optimized geometries of the triplet state and molecular orbitals of L-Cp; figures of the electron density distribution in contour plots of L-C_5H_4; and figures of the shapes of the deformation densities $\Delta\rho$ (PDF)

AUTHOR INFORMATION

Corresponding Author

Kartik Chandra Mondal − *Department of Chemistry, Indian Institute of Technology Madras, Chennai 600036, India;* orcid.org/0000-0002-5830-3608; Email: csdkartik@iitm.ac.in

Author

Sai Manoj N. V. T. Gorantla − *Department of Chemistry, Indian Institute of Technology Madras, Chennai 600036, India;* orcid.org/0000-0001-7315-6354

Complete contact information is available at: https://pubs.acs.org/10.1021/acsomega.1c00648

Notes

The authors declare no competing financial interest.

ACKNOWLEDGMENTS

We thank Prof. Gernot Frenking and Prof. K.M.S. for providing computational facilities. S.M. also thanks Dr. S. Pan. S.M. thanks CSIR for SRF. K.C.M. thanks SERB for the ECR grant (ECR/2016/000890) and IIT Madras for seed grant.

REFERENCES

(1) (a) Lewis, G. N. The Atom and the Molecule. *J. Am. Chem. Soc.* **1916**, *38*, 762. (b) Shaik, S. *Chem. − Eur. J.* **2007**, *28*, 51. (c) Güsten, R.; Wiesemeyer, H.; Neufeld, D.; Menten, K. M.; Graf, U. U.; Jacobs, K.; Klein, B.; Ricken, O.; Risacher, C.; Stutzki, J. Astrophysical detection of the helium hydride ion HeH^+. *Nature* **2019**, *568*, 357. (d) https://www.scientificamerican.com/article/the-first-molecule-in-the-universe/. (e) McCarthy, M. C.; Lee, K. L. K.; Loomis, R. A.; Burkhardt, A. M.; Shingledecker, C. N.; Charnley, S. B.; Cordiner, M. A.; Herbst, E.; Kalenskii, S.; Willis, E. R.; Xue, C.; Remijan, A. J.; McGuire, B. A. Interstellar detection of the highly polar five-membered ring cyanocyclopentadiene. *Nat. Astron.* **2021**, *5*, 176.

(2) (a) Evans, W. J. Tutorial on the Role of Cyclopentadienyl Ligands in the Discovery of Molecular Complexes of the Rare-Earth and Actinide Metals in New Oxidation States. *Organometallics* **2016**, *35*, 3088. (b) Mas-Roselló, J.; Herraiz, A. G.; Audic, B.; Laverny, A.; Cramer, N. Chiral Cyclopentadienyl Ligands: Design, Syntheses, and Applications in Asymmetric Catalysis. *Angew. Chem., Int. Ed.* **2020**, *59*, 2. (c) Fritz-Langhals, E. Silicon(II) Cation $Cp^*Si:^+ X^-$: A New Class of Efficient Catalysts in Organosilicon Chemistry. *Org. Process Res. Dev.* **2019**, *23*, 2369.

(3) (a) Trifonova, E. A.; Ankudinov, N. M.; Mikhaylov, A. A.; Chusov, D. A.; Nelyubina, Y. V.; Perekalin, D. S. A Planar-Chiral Rhodium(III) Catalyst with a Sterically Demanding Cyclopentadienyl Ligand and Its Application in the Enantioselective Synthesis of Dihydroisoquinolones. *Angew. Chem., Int. Ed.* **2018**, *57*, 7714. (b) Chena, W.-W.; Xu, M. -H. Recent advances in rhodium-catalyzed asymmetric synthesis of heterocycles. *Org. Biomol. Chem.* **2017**, *15*, 1029.

(4) Gould, C. A.; McClain, K. R.; Yu, J. M.; Groshens, T. J.; Furche, F.; Harvey, B. G.; Long, J. R. Synthesis and Magnetism of Neutral, Linear Metallocene Complexes of Terbium(II) and Dysprosium(II). *J. Am. Chem. Soc.* **2019**, *141*, 12967.

(5) (a) Arumugam, S.; Reddy, P. G.; Francis, M.; Kulkarni, A.; Roy, S.; Mondal, K. C. Highly fluorescent aryl-cyclopentadienyl ligands and their tetra-nuclear mixed metallic potassium−dysprosium clusters. *RSC Adv.* **2020**, *10*, 39366. (b) Roitershtein, D. M.; Puntus, L. N.; Vinogradov, A. A.; Lyssenko, K. A.; Minyaev, M. E.; Dobrokhodov, M. D.; Taidakov, I. V.; Varaksina, E. A.; Churakov, A. V.; Nifantév, I. E. Polyphenylcyclopentadienyl Ligands as an Effective Light-Harvesting π-Bonded Antenna for Lanthanide^{+3} Ions. *Inorg. Chem.* **2018**, *57*, 10199. (c) Yang, L.; Ye, J.; Xu, L.; Yang, X.; Gong, W.; Lin, Y.; Ning, G. Synthesis and properties of aggregation-induced emission enhancement compounds derived from triarylcyclopentadiene. *RSC Adv.* **2012**, *2*, 11529.

(6) (a) Wu, J.; Demeshko, S.; Decherta, S.; Meyer, F. Hexanuclear $[Cp^*Dy]_6$ single-molecule magnet. *Chem. Commun.* **2020**, *56*, 3887. (b) Guo, F.-S.; Day, B. M.; Chen, Y.-C.; Tong, M.-L.; Ki, A. M.; Layfield, R. A. A Dysprosium Metallocene Single-Molecule Magnet Functioning at the Axial Limit. *Angew. Chem., Int. Ed.* **2017**, *56*, 11445. (c) Guo, F.-S.; Day, B. M.; Chen, Y. C.; Tong, M.-L.; Mansikkamaki, A.; Layfield, R. A. Magnetic hysteresis up to 80 kelvin in a dysprosium metallocene single-molecule magnet. *Science* **2018**, *362*, 1400. (d) Goodwin, C. A. P.; Ortu, F.; Reta, D.; Chilton, N. F.; Mills, D. P. Molecular magnetic hysteresis at 60 kelvin in dysprosocenium. *Nature* **2017**, *548*, 439. (e) Moreno, L. E.; Baldovı, J. J.; Arino, A. G.; Coronado, E. Exploring the High-Temperature Frontier in Molecular Nanomagnets: From Lanthanides to Actinides. *Inorg. Chem.* **2019**, *58*, 11883. (f) Meihaus, K. R.; Fieser, M. E.; Corbey, J. F.; Evans, W. J.; Long, J. R. Record High Single-Ion Magnetic Moments Through $4f^n5d^1$ Electron Configurations in the Divalent Lanthanide Complexes $[(C_5H_4SiMe_3)_3Ln]^-$. *J. Am. Chem. Soc.* **2015**, *137*, 9855. (g) Demir, S.; Zadrozny, J. M.; Nippe, M.; Long, J. R. Exchange Coupling and Magnetic Blocking in Bipyrimidyl Radical-Bridged Dilanthanide Complexes. *J. Am. Chem. Soc.* **2012**, *134*, 18546.

(7) Demir, S.; Zadrozny, J. M.; Long, J. R. Large Spin-Relaxation Barriers for the Low-Symmetry Organolanthanide Complexes $[Cp^*_2Ln(BPh_4)]$ (Cp^*=pentamethylcyclopentadienyl; Ln=Tb, Dy). *Chem. − Eur. J.* **2014**, *20*, 9524.

(8) (a) Ramirez, F.; Levy, S. Communications - Triphenylphosphonium-cyclopentadienylide. *J. Org. Chem.* **1956**, *21*, 488. (b) Mueller-Westerhoff, U. Metallocenes from fulvenes: A new synthesis of functionally substituted ferrocenes. *Tetrahedron Lett.* **1972**, *13*, 4639. (c) Kunz, D.; Johnsen, E. Ø.; Monsler, B.; Rominger, F. Highly Ylidic Imidazoline-Based Fulvenes as Suitable Precursors for the Synthesis of Imidazolium-Substituted Metallocenes. *Chem. − Eur. J.* **2008**, *14*, 10909. (d) Schmid, D.; Seyboldt, A.; Kunz, D. A Direct Synthesis of a Strongly Zwitterionic 6,6'-Diaminofulvalene. *Z. Naturforsch. B* **2014**, *69*, 580. (e) Brownie, J.; Baird, M. Coordination complexes of aryl- and alkylphosphonium cyclopentadienylides (cyclopentadienylidene ylides), $C_5R_4PR'R''R'''$ (R = H, alkyl, aryl; R′, R′′, R′′′ = alkyl, aryl). *Coord. Chem. Rev.* **2008**, *252*, 1734. (g) Lin, R.; Zhang, H.; Li, S.; Wang, J.; Xia, H. New Highly Stable Metallabenzenes via Nucleophilic Aromatic Substitution Reaction. *Chem. − Eur. J.* **2011**, *17*, 4223. (h) Xu, C.; Wang, Z.-Q.; Li, Z.; Wang, W.-Z.; Hao, A.-Q.; Fu, W.-J.; Gong, J.-F.; Ji, B.-M.; Song, M.-P. 1,3-Diphosphorus Ylide Cyclopentadienylium Salts: Synthesis, Structures, and Application in Coupling Reactions. *Organometallics* **2012**, *31*, 798. (i) Schmid, D.; Seyboldt, A.; Kunz, D. Reaction of Iron-and Tungsten Carbonyls with a Zwitterionic Fulvalene. *Z. anorg. allg. Chem.* **2015**, *641*, 2228. (j) Schmid, D.; Seyboldt, A.; Eichele, K.; Kunz, D. Chiral amino-phosphine and amido-phosphine complexes of Ir and Mg. Catalytic applications in olefin hydroamination. *Dalton Trans.* **2016**, *45*, 12028. (k) Mazzotta, F.; Zitzer, G.; Speiser, B.; Kunz, D. Electron-Deficient Imidazolium Substituted Cp Ligands and their Ru Complexes. *Chem. − Eur. J.* **2020**, *26*, 16291.

(9) (a) Zhao, L.; Pan, S.; Holzmann, N.; Schwerdtfeger, P.; Frenking, G. Chemical Bonding and Bonding Models of Main-Group Compounds. *Chem. Rev.* **2019**, *119*, 8781. (b) Zhao, L.; Hermann, M.; Schwarz, W. H. E.; Frenking, G. The Lewis electron-pair bonding model: modern energy decomposition analysis. *Nat. Rev. Chem.* **2019**, *3*, 48. (c) Zhao, L.; von Hopffgarten, M.; Andrada, D. M.; Frenking, G. Energy Decomposition Analysis. *WIREs Comput. Mol. Sci.* **2018**, *8*, No. e1345.

(10) (a) Ramirez, F.; Desai, N. B.; Hansen, B.; McKelvie, N. HEXAPHENYLCARBODIPHOSPHORANE, $(C_6H_5)_3PCP(C_6H_5)_3$. *J. Am. Chem. Soc.* **1961**, *83*, 3539. (b) Tonner, R.; Frenking, G. $C(NHC)_2$: Divalent Carbon(0) Compounds with N-Heterocyclic Carbene Ligands—Theoretical Evidence for a Class of Molecules with Promising Chemical Properties. *Angew. Chem., Int. Ed.* **2007**, *46*, 8695. (c) Dyker, C. A.; Lavallo, V.; Donnadieu, B.; Bertrand, G. Synthesis of an Extremely Bent Acyclic Allene (A "Carbodicarbene"): A Strong Donor Ligand. *Angew. Chem., Int. Ed.* **2008**, *47*, 3206. (d) Fürstner, A.; Alcarazo, M.; Goddard, R.; Lehmann, C. W. Coordination Chemistry of Ene-1,1-diamines and a Prototype "Carbodicarbene". *Angew. Chem., Int. Ed.* **2008**, *47*, 3210. (e) Tonner, R.; Öxler, F.; Neumüller, B.; Petz, W.; Frenking, G. Carbodiphosphoranes: The Chemistry of Divalent Carbon(0). *Angew. Chem., Int. Ed.* **2006**, *45*, 8038.

(11) Gorantla, S. M. N. V. T.; Pan, S.; Mondal, K. C.; Frenking, G. Stabilization of Linear C_3 by Two Donor Ligands: A Theoretical Study of L-C_3-L (L=PPh_3, NHC^{Me}, $cAAC^{Me}$). *Chem. − Eur. J.* **2020**, *26*, 14211.

(12) (a) Sidgwick, N. V. *The Electronic Theory of Valency*, Clarendon, Oxford, 1927. (b) Himmel, D.; Krossing, I.; Schnepf, A. Dative Bonds in Main-Group Compounds: A Case for Fewer Arrows! *Angew. Chem., Int. Ed.* **2014**, *53*, 370. (c) Frenking, G. Dative Bonds in Main-Group Compounds: A Case for More Arrows! *Angew. Chem., Int. Ed.* **2014**, *53*, 6040. (d) Himmel, D.; Krossing, I.; Schnepf, A. Dative or Not Dative? *Angew. Chem., Int. Ed.* **2014**, *53*, 6047.

(13) (a) Varshavskii, Y. S. *Russ. J. Gen. Chem.* **1980**, *50*, 406. (b) Varshavskii, Y. S. Attempt to Describe Some Reactions of Organic Molecules Containing the R_1C Group in Terms of Donor-Acceptor Interaction. *Zh. Obshch. Khim.* **1980**, *50*, 514.

(14) (a) Becke, A. D. Density-functional exchange-energy approximation with correct asymptotic behavior. *Phys. Rev. A* **1988**, *38*, 3098. (b) Perdew, J. P. Density-functional approximation for the correlation energy of the inhomogeneous electron gas. *Phys. Rev. B* **1986**, *33*, 8822. (c) Grimme, S.; Ehrlich, S.; Goerigk, L. Effect of the damping function in dispersion corrected density functional theory. *J. Comput. Chem.* **2011**, *32*, 1456. (d) Grimme, S.; Antony, J.; Ehrlich, S.; Krieg, H. A consistent and accurate ab initio parametrization of density functional dispersion correction (DFT-D) for the 94 elements H-Pu. *J. Chem. Phys.* **2010**, *132*, 154104. (e) Weigend, F.; Ahlrichs, R. Balanced basis sets of split valence, triple zeta valence and quadruple zeta valence quality for H to Rn: Design and assessment of accuracy. *Phys. Chem. Chem. Phys.* **2005**, *7*, 3297. (f) Weigend, F. Accurate Coulomb-fitting basis sets for H to Rn. *Phys. Chem. Chem. Phys.* **2006**, *8*, 1057.

(15) *Gaussian 16, Revision A.03*, Frisch, M. J., et al. Gaussian, Inc., Wallingford CT. 2016.

(16) (a) Weinhold, F.; Landis, C. *Valency and Bonding, A Natural Bond Orbital Donor − Acceptor Perspective,* Cambridge University Press, Cambridge, 2005. (b) Landis, C. R.; Weinhold, F. *The NBO View of Chemical Bonding, in,* G., Frenking, S., Shaik *(eds.), The Chemical Bond: Fundamental Aspects of Chemical Bonding.* Wiley, 2014, pp. 91−120. (c) Bickelhaupt, F. M.; Baerends, E. J. Kohn-Sham Density Functional Theory: Predicting and Understanding Chemistry. In *Rev. Comput. Chem.*; Lipkowitz, K. B., Boyd, D. B., Eds.; Wiley-VCH: New York, 2000; Vol. *15*, pp. 1−86.

(17) Wiberg, K. B. Application of the pople-santry-segal CNDO method to the cyclopropylcarbinyl and cyclobutyl cation and to bicyclobutane. *Tetrahedron* **1968**, *24*, 1083.

https://doi.org/10.1021/acsomega.1c00648
ACS Omega 2021, 6, 17798−17810

(18) Glendening, E. D.; Landis, C. R.; Weinhold, F. NBO 6.0: Natural bond orbital analysis program. *J. Comput. Chem.* **2013**, *34*, 1429.
(19) Ziegler, T.; Rauk, A. On the calculation of bonding energies by the Hartree Fock Slater method. *Theor. Chim. Acta* **1977**, *46*, 1.
(20) (a) Mitoraj, M.; Michalak, A. Donor−Acceptor Properties of Ligands from the Natural Orbitals for Chemical Valence. *Organometallics* **2007**, *26*, 6576. (b) Mitoraj, M.; Michalak, A. Applications of natural orbitals for chemical valence in a description of bonding in conjugated molecules. *J. Mol. Model.* **2008**, *14*, 681.
(21) (a) *ADF2017*, SCM, Theoretical Chemistry, Vrije Universiteit, Amsterdam, The Netherlands, http://www.scm.com; (b) te Velde, G.; Bickelhaupt, F. M.; Baerends, E. J.; Guerra, C. F.; van Gisbergen, S. J. A.; Snijders, J. G.; Ziegler, T. Chemistry with ADF. *J. Comput. Chem.* **2001**, *22*, 931.
(22) (a) van Lenthe, E.; Baerends, E. J. Optimized Slater-type basis sets for the elements 1−118. *J. Comput. Chem.* **2003**, *24*, 1142. (b) van Lenthe, E.; Baerends, E. J.; Snijders, J. G. Relativistic regular two-component Hamiltonians. *J. Chem. Phys.* **1993**, *99*, 4597. (c) van Lenthe, E.; Baerends, E. J.; Snijders, J. G. Relativistic total energy using regular approximations. *J. Chem. Phys.* **1994**, *101*, 9783.
(23) (a) Frenking, G.; Bickelhaupt, F. M. *The Chemical Bond 1. Fundamental Aspects of Chemical Bonding*, chap. The EDA Perspective of Chemical Bonding, 121. Wiley-VCH: Weinheim, 2014. (b) Zhao, L. M.; von Hopffgarten; Andrada, D. M.; Frenking, G. *WIREs Comput. Mol. Sci.* **2018**, *8*, 1345. (c) Zhao, L.; Hermann, M.; Schwarz, W. H. E.; Frenking, G. The Lewis electron-pair bonding model: modern energy decomposition analysis. *Nat. Rev. Chem.* **2019**, *3*, 48. (d) Yang, W.; Krantz, K. E.; Freeman, L. A.; Dickie, D.; Molino, A.; Frenking, G.; Pan, S.; Wilson, D. J. D.; Gilliard, R. J., Jr. Persistent Borafluorene Radicals. *Angew. Chem., Int. Ed.* **2020**, *59*, 3850. (e) Deng, G.; Pan, S.; Wang, G.; Zhao, L.; Zhou, M.; Frenking, G. Side-On Bonded Beryllium Dinitrogen Complexes. *Angew. Chem., Int. Ed.* **2020**, *59*, 10603. (f) Pan, S.; Frenking, G. Comment on "Realization of Lewis Basic Sodium Anion in the $NaBH_3$− Cluster". *Angew. Chem., Int. Ed.* **2020**, *59*, 8756. (g) Zhao, L.; Pan, S.; Zhou, M.; Frenking, G. Response to Comment on "Observation of alkaline earth complexes $M(CO)_8$ (M = Ca, Sr, or Ba) that mimic transition metals". *Science* **2019**, *365*, No. eaay5021. (h) Saha, R.; Pan, S.; Chattaraj, P. K.; Merino, G. Filling the void: controlled donor−acceptor interaction facilitates the formation of an M−M single bond in the zero oxidation state of M (M = Zn, Cd, Hg). *Dalton Trans.* **2020**, *49*, 1056.
(24) (a) Andrés, J.; Ayers, P. W.; Boto, R. A.; Carbó-Dorca, R.; Chermette, H.; Cioslowski, J.; Contreras-García, J.; Cooper, D. L.; Frenking, G.; Gatti, C.; Heidar-Zadeh, F.; Joubert, L.; Martín Pendás, A.; Matito, E.; Mayer, I.; Misquitta, A. J.; Mo, Y.; Pilmé, J.; Popelier, P. L. A.; Rahm, M.; Ramos-Cordoba, E.; Salvador, P.; Schwarz, W. H. E.; Shahbazian, S.; Silvi, B.; Solà, M.; Szalewicz, K.; Tognetti, V.; Weinhold, F.; Zins, E. L. Nine questions on energy decomposition analysis. *J. Comput. Chem.* **2019**, *40*, 2248.
(25) (a) Yufit, D. S.; Howard, J. A. K.; Davidson, M. G. Bonding in phosphorus ylides: topological analysis of experimental charge density distribution in triphenylphosphonium benzylide. *J. Chem. Soc., Perkin Trans.* **2000**, *2*, 249. (b) Kulkarni, A.; Arumugam, S.; Francis, M.; Reddy, P. G.; Nag, E.; Gorantla, S. M. N. V. T.; Mondal, K. C.; Roy, S. Solid-State Isolation of Cyclic Alkyl(Amino) Carbene (cAAC)-Supported Structurally Diverse Alkali Metal-Phosphinidenides. *Chem. − Eur. J.* **2021**, *27*, 200.
(26) Lloyd, D.; Sneezum, J. S. The preparation of some pyridinium cyclopentadienylides. *Tetrahedron* **1958**, *14*, 334.
(27) (a) Matta, C. F.; Boyd, R. J. *The Quantum Theory of Atoms in Molecules: From Solid State to DNA and Drug Design (Eds.:), Chapter 1. An Introduction to the Quantum Theory of Atoms in Molecules*, Wiley: Hoboken, 2007, 1; (b) Bader, R. F. W. *Acc. Chem. Res.* **1985**, *18*, 9. (c) Bader, R. F. W. *Chem. Rev.* **1991**, *94*, 893. (d) Kumar, P. S. V.; Raghavendra, V.; Subramanian, V. *J. Chem. Sci.* **2016**, *128*, 1527.
(28) (a) Zhang, Q.; Li, W. -L.; Xu, C.; Chen, M.; Zhou, M.; Li, J.; Andrada, D. M.; Frenking, G. Formation and Characterization of the Boron Dicarbonyl Complex $[B(CO)_2]^-$. *Angew. Chem., Int. Ed.* **2015**, *54*, 11078. (b) Andrada, D. M.; Frenking, G. Stabilization of Heterodiatomic SiC Through Ligand Donation: Theoretical Investigation of $SiC(L)_2$ (L=NHC^{Me}, $CAAC^{Me}$, PMe_3). *Angew. Chem., Int. Ed.* **2015**, *54*, 12319. (c) Mohapatra, C.; Kundu, S.; Paesch, A. N.; Herbst-Irmer, R.; Stalke, D.; Andrada, D. M.; Frenking, G.; Roesky, H. W. The Structure of the Carbene Stabilized Si_2H_2 May Be Equally Well Described with Coordinate Bonds as with Classical Double Bonds. *J. Am. Chem. Soc.* **2016**, *138*, 10429. (d) Scharf, L. T.; Andrada, D. M.; Frenking, G.; Gessner, V. H. The Bonding Situation in Metalated Ylides. *Chem. − Eur. J.* **2017**, *23*, 4422. (e) Hermann, M.; Frenking, G. Carbones as Ligands in Novel Main-Group Compounds $E[C(NHC)_2]_2$ (E=Be, B^+, C^{2+}, N^{3+}, Mg, Al^+, Si^{2+}, P^{3+}): A Theoretical Study. *Chem. − Eur. J.* **2017**, *23*, 3347. (f) Georgiou, D. C.; Zhao, L.; Wilson, D. J. D.; Frenking, G.; Dutton, J. L. NHC-Stabilised Acetylene—How Far Can the Analogy Be Pushed? *Chem. − Eur. J.* **2017**, *23*, 2926.
(29) (a) Dewar, M. J. S. A Review of the π-Complex Theory. *Bull. Soc. Chim. Fr.* **1951**, *18*, C79. (b) Chatt, J.; Ducanson, L. A. J. Olefin co-ordination compounds. Part III. Infra-red spectra and structure: attempted preparation of acetylene complexes. *Chem. Soc.* **1953**, 2929.
(30) (a) Schleyer, P. v. R.; Maerker, C.; Dransfeld, A.; Jiao, H.; Hommes, N. J. R. v. E. Nucleus-Independent Chemical Shifts: A Simple and Efficient Aromaticity Probe. *J. Am. Chem. Soc.* **1996**, *118*, 6317. (b) Chen, Z.; Wannere, C. S.; Corminboeuf; Puchta, R.; Schleyer, P. v. R. Nucleus-Independent Chemical Shifts (NICS) as an Aromaticity Criterion. *Chem. Rev.* **2005**, *105*, 3842.
(31) Baryshnikov, G. V.; Minaev, B. F.; Pittelkow, M.; Nielsen, C. B.; Salcedo, R. Nucleus-independent chemical shift criterion for aromaticity in π-extended tetraoxa[8]circulenes. *J. Mol. Model.* **2013**, *19*, 847.

https://doi.org/10.1021/acsomega.1c00648
ACS Omega 2021, 6, 17798−17810